

Synchronization of Delay-coupled Micromechanical Oscillators

Shreyas Y. Shah,¹ Mian Zhang,² Richard Rand,^{3,4} and Michal Lipson^{1,5,6}

¹*School of Electrical and Computer Engineering,
Cornell University, Ithaca, New York 14853, USA*

²*School of Engineering and Applied Sciences, Harvard University, Cambridge, Massachusetts 02138, USA*

³*Department of Mathematics, Cornell University, Ithaca, New York 14853, USA*

⁴*Sibley School of Mechanical and Aerospace Engineering,
Cornell University, Ithaca, New York 14853, USA*

⁵*Kavli Institute at Cornell for Nanoscale Science, Ithaca, New York 14853, USA*

⁶*Department of Electrical Engineering, Columbia University, New York, New York 10027, USA*

Delay-coupled oscillators exhibit unique phenomena that are not present in systems without delayed coupling. In this paper, we experimentally demonstrate mutual synchronisation of two free-running micromechanical oscillators, coupled via light with a total delay 139 ns which is approximately four and a half times the mechanical oscillation time period. This coupling delay, imposed by a finite speed of propagation of light, induces multiple stable states of synchronised oscillations, each with a different oscillation frequency. These states can be accessed by varying the coupling strengths. Our result could enable applications in reconfigurable radio-frequency networks, and novel computing concepts.

PACS numbers: 05.45.Xt, 07.10.Cm, 42.82.Et

Time-delay in coupled systems is ubiquitous in nature because of the finite propagation speed of any signal, and because of the finite response time of physical systems (e.g. neuronal networks [1, 2], chemical reactions [3], biochemical systems [4–7]). Delayed-coupling can significantly influence the behaviour of coupled systems [1–6, 8–14]. In particular, for two coupled oscillators, the presence of a time-delay could enable a multitude of stable states of synchronised oscillations [4, 5, 8, 9, 11, 12]. Recently, synchronisation of micromechanical oscillators has attracted a lot of attention [15–25] due to potential applications in communication [26], signal-processing [27], as well as in novel complex networks [17, 28]. However, effects of delayed-coupling have not yet been experimentally demonstrated on this technologically important platform.

A major challenge is to effectively introduce significant time-delay in systems of coupled micromechanical oscillators. Existing schemes [15, 16, 21–24] for mutual synchronisation require the micromechanical oscillators to be in physical proximity, restricting the types of coupled-dynamics that the system can exhibit. Micromechanical oscillators can interact via electronic coupling [23, 24] or elastic coupling [15], both of which are fundamentally lossy and require the oscillators to be separated by a distance much smaller than their oscillation wavelengths, thereby rendering the time-delay insignificant.

Coupling micromechanical oscillators via light can help overcome the limitation of distance, since light can propagate with negligible loss over long distances [29]. Light-mediated mutual synchronization of micromechanical oscillators that has been demonstrated thus far [16, 21, 22]

has been with optomechanical oscillators (OMOs) that interact via a common optical microresonator, which requires them to be separated by only a few microns.

In this work, we synchronise two independent OMOs by mutually coupling them with an effective delay of approximately 4.5 times their oscillation time period. This scheme is based on using the radio-frequency (RF) oscillations of one oscillator to modulate the optical drive, and thereby influence the time-evolution of the phase of oscillations of the other oscillator, and vice-versa [30]. Each OMO can be modelled as a mechanical oscillator (Eq. 1), with natural frequency Ω and damping rate Γ . It is driven into self-sustained, free running, oscillations by a position-dependent ($x(t)$) optical force $F_{opt}(x(t))$, provided by a continuous wave laser [31]. This force on one OMO is modulated by the mechanical displacement signal of the other OMO (and vice-versa) $x(t - T)$ after a propagation delay of T and a coupling-constant γ . Therefore, $T \approx 4.5 \times 2\pi/\Omega$. See Supplemental Material for details.

$$\ddot{x}_{i,j}(t) + \Gamma \dot{x}_{i,j}(t) + \Omega_{i,j}^2 x_{i,j}(t) = F_{opt\ i,j}(x_{i,j}(t)) [1 + \gamma_{ij,ji} x_{j,i}(t - T)] \quad (1)$$

Each oscillator used in this experiment has a double micro-disk structure (Fig. 1), that supports coupled optical and mechanical resonances, and is driven into self-sustained, free running, oscillations with an external laser. The double micro-disk structure is composed of two, vertically stacked, suspended microdisks with a spacer between them (Fig. 1(a)). The top and bottom disks are made of low-pressure chemical vapour deposition (CVD) grown Si_3N_4 , and are nominally 248 nm and 220 nm thick, respectively. The spacer is made of 170

nm thick plasma-enhanced CVD grown SiO₂. This stack rests on a 4 μm thick substrate of thermally grown SiO₂. These thin films were patterned into disks with a 20 μm radius using electron-beam lithography and inductively-coupled reactive ion etching. The SiO₂ layers are partially etched away with buffered hydrofluoric acid to release the periphery of the disks (Fig. 1(b)). The resultant structure supports a high-quality-factor whispering gallery optical mode that is coupled to the out-of-phase mechanical resonance of the two disks (Fig. 1(a)). The coupling strength between the optical and mechanical degrees of freedom is characterised by the optomechanical coupling-constant $G_{\text{om}} = -2\pi \times 45$ GHz/nm, as deduced from finite element simulations [16].

We optically couple two OMOs with individual mechanical oscillation frequencies of 32.9 MHz and 32.97 MHz with a total delay of 139 ns (effective distance of 28.5 m) between them. The delay between the two oscillators is introduced using low loss optical fibres, which propagate the transmitted optical signal over a distance (Fig. 2). The RF oscillations of OMO 1 (Fig. 2) are carried by light over the optical delay line, and converted to an electrical signal at a high-speed photodetector. This electrical signal modulates the power of the laser driving OMO 2 (using an electro-optic modulator, EOM 2), thereby coupling OMO 1 to OMO 2. Similarly, OMO 2 couples to OMO 1 via EOM 1.

The strength of this coupling is controlled with a variable-gain RF amplifier (VGA 1,2), that can provide an arbitrary gain between -26 dB and +35 dB. The coupling strengths κ_{ij} ($i,j = 1,2$) are defined as $\kappa_{ij} = \frac{H_{in,j,i}}{H_{osc,j}}$, where $H_{osc,j}$ is the oscillation power of OMO 'j', and $H_{in,j,i}$ is the power of the signal from OMO 'i' imparted on the laser (via EOM 'j') driving OMO 'j'. κ_{12} is controlled by VGA 1 and κ_{21} is controlled by VGA 2. The ratio $\frac{\kappa_{12}}{\kappa_{21}}$ is kept fixed, using a third VGA (not shown in schematic in Fig. 2).

We show that the two oscillators transition from oscillating independently to oscillating in a synchronised manner at an intermediate frequency as we increase the coupling strength. When the oscillators are weakly coupled (small values of κ_{12} , κ_{21}), they oscillate at their individual frequencies (Fig. 3). As the coupling strength is increased, we observe frequency-pulling [20, 32] i.e. the frequencies of the two oscillators are pulled towards each other, while they still oscillate independently, prior to the onset of synchronised oscillations. As the coupling strength is increased beyond a threshold value, (κ_{21}, κ_{12}) (-10.5 dB, -4.1 dB), (-12.13 dB, 1.5 dB) for Figs. 3(a) and 3(b) respectively, the two oscillators spontaneously

begin to oscillate in synchrony, as indicated by the emergence of a single RF tone in the transmitted optical power spectrum.

We demonstrate that these OMOs also exhibit multiple stable states in which they oscillate synchronously, as opposed to just a single stable synchronised state seen in systems without delay [8, 9, 11]. The different stable synchronised oscillations, which have different frequencies, can be accessed by selecting appropriate values for the coupling constants, κ_{21} and κ_{12} , which determine the strength with which OMO 2 couples to OMO 1, and vice versa. For instance, as shown in Fig. 3(a) ($\frac{\kappa_{12}}{\kappa_{21}} = 6.32$ dB) not only do the two oscillators synchronise ($\kappa_{21} = -10.5$ dB) but also a second synchronisation frequency is seen merely by increasing κ_{21} further ($\kappa_{21} = -6.5$ dB). Similarly, for $\frac{\kappa_{12}}{\kappa_{21}} = 13.63$ dB (Fig. 3(b)), we see three synchronised states beyond the synchronisation threshold.

Interestingly, the frequencies of the synchronised states vary in discrete steps in a manner similar to what is also found in other delay-coupled systems [11, 12]. For any given ratio κ_{12}/κ_{21} , as the coupling strength is increased, the two oscillators initially synchronise at a frequency close to the average of their natural oscillation frequencies (Fig. 3). Further increase in the coupling strength gives synchronised states with frequencies that span the difference between the two natural frequencies in discrete steps.

This demonstration of controllable, multi-stable synchronisation between delay-coupled OMOs paves the way towards implementing novel memory and communication concepts [17, 26]. Delayed-coupling enables us to choose from multiple possible synchronised states, which have different oscillation frequencies enabling applications of OMOs in distributed, reconfigurable communication networks. Delayed coupling also manifests itself in biological systems [4, 5, 7], particularly neuronal networks [1, 2, 6]. This demonstration of synchronisation of OMOs showcases a microscopic, scalable platform that could potentially be used to implement various schemes of neuromorphic information processing and computation [17, 33, 34].

-
- [1] G. Deco, V. Jirsa, A. R. McIntosh, O. Sporns, and R. Ktter, Proceedings of the National Academy of Sciences **106**, 10302 (2009).
 - [2] M. Dhamala, V. K. Jirsa, and M. Ding, Physical Review Letters **92**, 074104 (2004).
 - [3] T. Erneux and J. Grasman, Physical Review E **78**, 026209 (2008).
 - [4] A. Takamatsu, T. Fujii, and I. Endo, Physical Review Letters **85**, 2026 (2000).
 - [5] A. Takamatsu, Physica D: Nonlinear Phenomena **223**, 180 (2006).
 - [6] E. Rossoni, Y. Chen, M. Ding, and J. Feng, Physical Review E **71**, 061904 (2005).

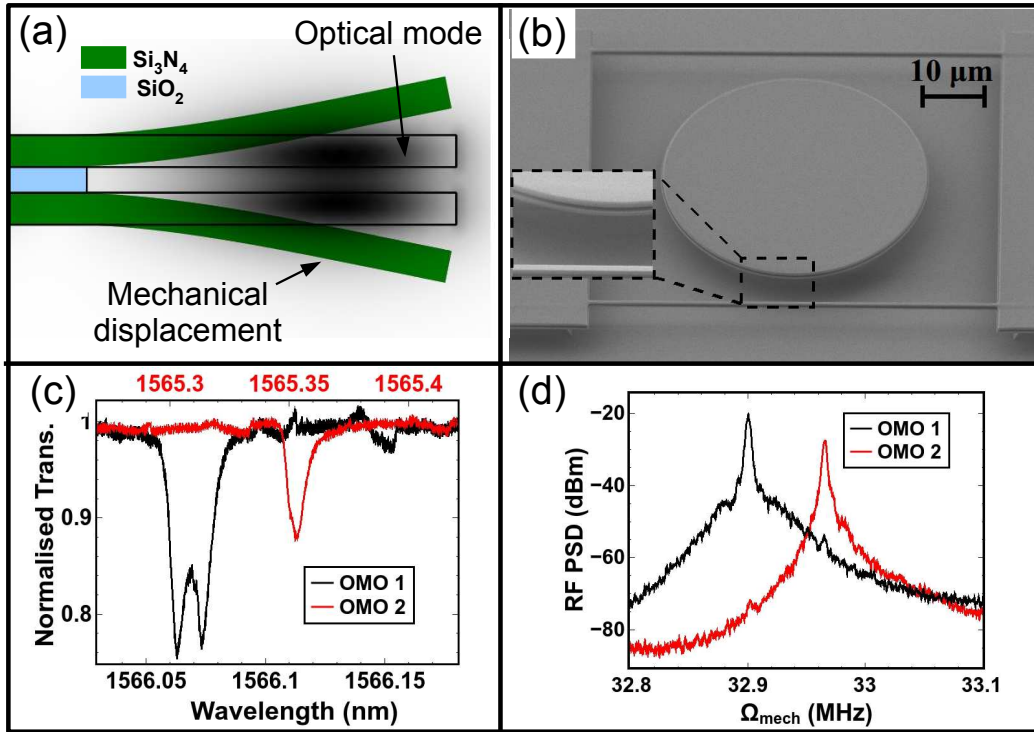


Figure 1. (a) Schematic cross-sectional picture of the periphery of a typical optomechanical (OM) resonator, indicating the localisation of optical and mechanical modes. (b) SEM image of a typical double-disk OM resonator, surrounded by a structure to support tapered optical fibers used to optically excite mechanical oscillations. (Inset) Higher-magnification image of the double micro-disk structure (c) Normalised optical transmission spectra of the two OM resonators used in this demonstration. (d) Power spectrum of the transmitted optical power modulated as each device is driven into self-sustained oscillations. The oscillation frequencies are separated by 70 kHz.

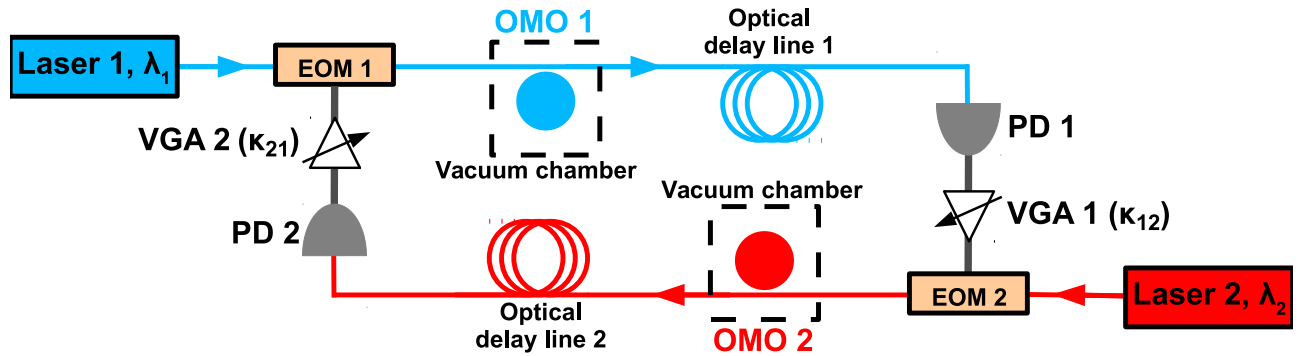


Figure 2. Schematic of experimental setup to synchronise two optomechanical oscillators (OMOs). Each device is driven by an independent laser tuned to be blue-side of its optical resonance. The transmitted optical signals, modulated by each OMO, travel over 9 m long delay line of SMF-28 optical fibres. The RF signal generated at the photodetector (PD) at the end of optical delay line 1 modulates the power of the laser driving OMO 2 via an electro-optic modulator (EOM), and vice-versa. The strengths of these modulation signals are controlled by variable-gain RF amplifiers (VGA). Half of the RF oscillation signal is tapped off at each of the photodetector for analysing with an RF spectrum analyser (See Supplemental material for a more detailed schematic).

- [7] S. Kauffman and J. J. Wille, *Journal of Theoretical Biology* **55**, 47 (1975).
 [8] M. Y. Choi, H. J. Kim, D. Kim, and H. Hong, *Physical Review E* **61**, 371 (2000).
 [9] S. Kim, S. H. Park, and C. S. Ryu, *Physical Review Letters* **79**, 2911 (1997).
 [10] D. V. Ramana Reddy, A. Sen, and G. L. Johnston, *Physical Review Letters* **80**, 5109 (1998).
 [11] H. G. Schuster and P. Wagner, *Progress of Theoretical Physics* **81**, 939 (1989).
 [12] H.-J. Wnsche, S. Bauer, J. Kreissl, O. Ushakov, N. Korneyev, F. Henneberger, E. Wille, H. Erz-

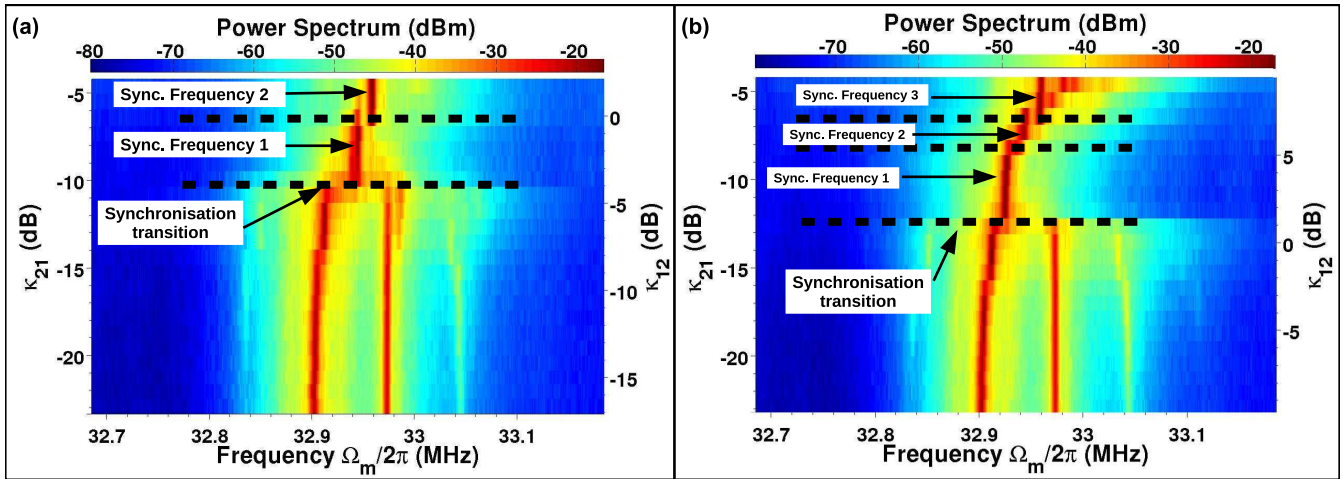


Figure 3. Combined power spectrum of the transmitted optical power of the two OMOs, as a function of increasing coupling strengths κ_{21} (κ_{12}), showing the synchronisation transition, while κ_{12}/κ_{21} is kept constant at (a) 6.32 dB and (b) 13.63 dB. As κ_{21} and κ_{12} are increased beyond the synchronisation threshold, we see (a) 2 synchronised states and (b) 3 synchronised states, respectively.

- grber, M. Peil, W. Elser, and I. Fischer, *Physical Review Letters* **94**, 163901 (2005).
- [13] S. Yanchuk, *Physical Review E* **72**, 036205 (2005).
- [14] S. Warkus and R. Rand, *Nonlinear Dynamics* **30**, 205 (2002).
- [15] S.-B. Shim, M. Imboden, and P. Mohanty, *Science* **316**, 95 (2007).
- [16] M. Zhang, G. S. Wiederhecker, S. Manipatruni, A. Barnard, P. McEuen, and M. Lipson, *Physical review letters* **109**, 233906 (2012).
- [17] F. Hoppensteadt and E. Izhikevich, *IEEE Transactions on Circuits and Systems I: Fundamental Theory and Applications* **48**, 138 (2001).
- [18] C. A. Holmes, C. P. Meaney, and G. J. Milburn, *Physical Review E* **85**, 066203 (2012).
- [19] G. Len Aveleyra, C. A. Holmes, and G. J. Milburn, *Physical Review E* **89**, 062912 (2014).
- [20] M. C. Cross, A. Zumdieck, R. Lifshitz, and J. L. Rogers, *Physical Review Letters* **93**, 224101 (2004).
- [21] M. Zhang, S. Shah, J. Cardenas, and M. Lipson, *Physical Review Letters* **115**, 163902 (2015).
- [22] M. Bagheri, M. Poot, L. Fan, F. Marquardt, and H. X. Tang, *Physical Review Letters* **111**, 213902 (2013).
- [23] M. H. Matheny, M. Grau, L. G. Villanueva, R. B. Karabalin, M. Cross, and M. L. Roukes, *Physical Review Letters* **112**, 014101 (2014).
- [24] D. K. Agrawal, J. Woodhouse, and A. A. Seshia, *Physical Review Letters* **111**, 084101 (2013).
- [25] G. Heinrich, M. Ludwig, J. Qian, B. Kubala, and F. Marquardt, *Physical Review Letters* **107**, 043603 (2011).
- [26] S. Bregni, *Synchronization of Digital Telecommunications Networks* (Wiley, 2002).
- [27] K. Stephan, *IEEE Transactions on Microwave Theory and Techniques* **49**, 138 (2001).
- [28] M. C. Soriano, J. Garca-Ojalvo, C. R. Mirasso, and I. Fischer, *Reviews of Modern Physics* **85**, 421 (2013).
- [29] R. B. Karabalin, M. Cross, and M. L. Roukes, *IEEE Transactions on Microwave Theory and Techniques* **49**, 138 (2001).
- [30] S. Y. Shah, M. Zhang, R. Rand, and M. Lipson, *Physical Review Letters* **114**, 113602 (2015).
- [31] T. J. Kippenberg and K. J. Vahala, *Optics Express* **15**, 17172 (2007).
- [32] B. Razavi, *IEEE Journal of Solid-State Circuits* **39**, 1415 (2004).
- [33] M. Lee, A. Hirose, Z.-G. Hou, and R. M. Kil, *Neural Information Processing: 20th International Conference, ICONIP 2013, Daegu, Korea, November 3-7, 2013. Proceedings* (Springer, 2013).
- [34] J. Cosp, J. Madrenas, E. Alarcon, E. Vidal, and G. Villar, *IEEE Transactions on Neural Networks* **15**, 1315 (2004).

Synchronization of Delay-coupled Micromechanical Oscillators

Shreyas Y. Shah,¹ Mian Zhang,² Richard Rand,^{3,4} and Michal Lipson^{1,5,6}

¹*School of Electrical and Computer Engineering,
Cornell University, Ithaca, New York 14853, USA*

²*School of Engineering and Applied Sciences,
Harvard University, Cambridge, Massachusetts 02138, USA*

³*Department of Mathematics, Cornell University, Ithaca, New York 14853, USA*

⁴*Sibley School of Mechanical and Aerospace Engineering,
Cornell University, Ithaca, New York 14853, USA*

⁵*Kavli Institute at Cornell for Nanoscale Science, Ithaca, New York 14853, USA*

⁶*Department of Electrical Engineering,
Columbia University, New York, New York 10027, USA*

EXPERIMENTAL SETUP AND PROCEDURE FOR DELAY-COUPLED SYNCHRONISATION

A more detailed schematic of experimental setup to synchronise two optomechanical oscillators (OMOs) is shown in Fig. 1. As described in the main text, each device is driven by an independent laser tuned to be blue-side of its optical resonance. The transmitted optical signals, modulated by each OMO, travel over delay line of SMF-28 optical fibres. The RF signal generated at the photodetectors (DC filters are used to block the DC signal) at the end of optical delay lines modulate the power of the lasers driving the two OMOs via electro-optic modulators (EOM). The strengths of these modulation signals are controlled by variable-gain RF amplifiers (VGA).

The coupling strengths are primarily determined by VGA1 and VGA2. The two OMOs are first pumped into self-sustained oscillations, while keeping the gain values very low (< -20 dB), so that the two devices oscillate independently. VGA1 and VGA2 are controlled by the same voltage source, and have the same gain (within their specifications) as the control-voltage is varied. The synchronisation transition i.e. when the two OMOs transition from independent oscillations at different frequencies to locked oscillations at the same frequency, is seen when the gain is increased. We increase the gain in steps of ≈ 0.9 dB.

Half of the RF oscillation signal is tapped off at each of the photodetector for analysing with an RF spectrum analyser. Since the instrument we use only has a single input channel, we analyse and record the spectrum of each oscillator independently. Therefore, each voltage scan (as described in the previous paragraph) is performed twice, first to record the output of Splitter 1 and then to record the output of Splitter 2. The two spectra are then mathematically added using numerical software to yield a combined RF spectrum for the two OMOs.

We have seen earlier [1] that the response of an OMO to an externally injected periodic signal is highly asymmetric with respect to the detuning between the OMO and the external signal. Therefore, an OMO is more susceptible to locking by an external signal if that signal has a higher frequency than if it has a lower frequency. This means that, in order to observe synchronisation dynamics, it is not enough to have equal values of gain (and thereby κ_{21} and κ_{12}).

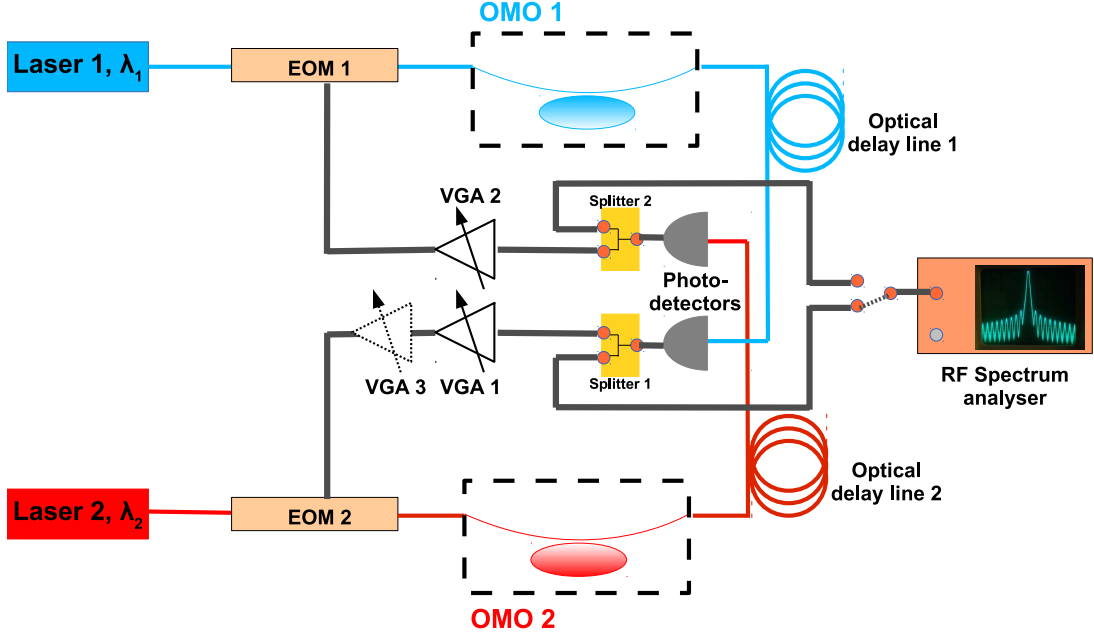


Figure 1. Detailed experimental schematic

A third amplifier VGA3, cascaded with VGA1 and controlled independently of VGA1 and VGA2, is used to differentiate between κ_{21} and κ_{12} . The gain of VGA3 is kept fixed throughout the voltage-scan described above.

MATHEMATICAL MODEL FOR DELAYED COUPLING

Each OMO can be modelled as a pair of parametrically coupled optical (Eq. S1) and mechanical (Eq. S2) resonators, where a is the electric field strength in the optical resonator, such that $|a|^2$ is the energy stored in the cavity, Δ_0 is the detuning between the laser frequency and the resonance frequency of the optical cavity ω , Γ_{opt} is the optical decay rate, Γ_{ext} is the rate at which laser power $|s|^2$ is coupled into the optical cavity from the tapered fiber, G_{om} is the optomechanical coupling coefficient and m_{eff} is the effective mass of the mechanical resonator. The rest of the parameters are described in the main text.

$$\frac{da}{dt} = i(\Delta_0 - G_{om}x)a - \Gamma_{opt}a + \sqrt{2\Gamma_{ext}}s \quad (S1)$$

$$\frac{d^2x}{dt^2} + \Gamma_m \frac{dx}{dt} + \Omega_m^2 x = \frac{G_{om}|a|^2}{m_{eff}\omega} \quad (S2)$$

For the OMOs that we used in this demonstration of synchronisation, the optical de-

cay rate Γ_{opt} is much larger than the mechanical frequency Ω_m , and Eqs. S1, S2 can be approximated by a single equation Eq. S3, where τ is the response time of the optical cavity.

$$\frac{d^2x(t)}{dt^2} + \Gamma_m \frac{dx(t)}{dt} + \Omega_m^2 x(t) = \frac{2G_{om}\Gamma_{ex}}{m_{eff}\omega} \frac{1}{(\Delta_0 - G_{om}x(t - \tau))^2 + \Gamma_{opt}^2} |s|^2 \quad (\text{S3})$$

The laser power $|s|^2$ driving one OMO is modulated, via an electro-optic modulator, by the RF oscillation signal of the other OMO, P_{trans} (Eq. S4) ([1], Supplementary). Here, $\frac{\Gamma}{2}$ represents the strength of modulation due to P_{trans} .

$$|s|^2 = |s_0|^2 \left(1 + \frac{\Gamma}{2} P_{trans}\right) \quad (\text{S4})$$

P_{trans} is the RF oscillation power of the OMO, that modulates the laser power $|s|^2$. It can be shown that $P_{trans}(t) \propto x_{trans}(t)$ [1]. Substituting this in Eq. S4, and combining it with S3, assuming that P_{trans} is delayed by T , we get Eq. S5, which describes the delayed coupling between the two OMOs.

$$\frac{d^2x(t)}{dt^2} + \Gamma_m \frac{dx(t)}{dt} + \Omega_m^2 x(t) = F_{opt}(x(t))(1 + \gamma x_{trans}(t - T)) \quad (\text{S5})$$

where, $F_{opt}(x(t)) = \frac{2G_{om}\Gamma_{ex}}{m_{eff}\omega} \frac{1}{(\Delta_0 - G_{om}x(t - \tau))^2 + \Gamma_{opt}^2} |s_0|^2$

[1] S. Y. Shah, M. Zhang, R. Rand, and M. Lipson, Physical Review Letters **114**, 113602 (2015).